Pergamon

Geochimica et Cosmochimica Acta, Vol. 68, No. 22, pp. 4559-4569, 2004

0016-7037/04 $30.00 + .00

doi:10.1016/j.gca.2004.04.012

Pyrite dissolution in acidic media

M. DESCOSTES,* P. VITORGE, and C. BEAUCAIRE†
CEA, DEN Saclay, DPC/SECR/L3MR, CEN, F-91191 Gif-sur-Yvette, France

(*Received July* 28, 2003; *accepted in revised form April* 8, 2004)

Abstract—Oxidation of pyrite in aqueous solutions in contact with air (oxygen 20%) was studied at 25°C using short-term batch experiments. Fe^{2+} and SO_4^{2-} were the only dissolved Fe and S species detected in these solutions. After a short period, $R = [S]_{tot}/[Fe]_{tot}$ stabilized from 1.25 at pH = 1.5 to 1.6 at pH = 3. These R values were found to be consistent with previously published measurements (as calculated from the raw published data). This corresponds to a nonstoichiometric dissolution ($R < 2$) resulting from a deficit in aqueous sulfur. Thermodynamics indicate that S(−I) oxidation can only produce $S^0_{(s)}$ and SO_4^{2-} under these equilibrium conditions. However, Pourbaix diagrams assuming the absence of SO_4^{2-} indicate that $S_2O_3^{2-}$ and $S_4O_6^{2-}$ can appear in these conditions. Using these species the simplest expected oxidation mechanism is

$$FeS_{2(s)} + 1.5O_2 \rightarrow Fe^{2+} + S_2O_3^{2-}$$

followed by

$$S_2O_3^{2-} + 1.2H^+ \rightarrow 0.4S^0_{(s)} + 0.4S_4O_6^{2-} + 0.6H_2O,$$

and finally

$$S_4O_6^{2-} + 3.5O_2 + 3H_2O \rightarrow 4SO_4^{2-} + 6H^+$$

possibly in several steps

The overall reaction is

$$FeS_2 + 2.9O_2 + 0.6H_2O \rightarrow Fe^{2+} + 0.4S^0_{(s)} + 1.6SO_4^{2-} + 1.2H^+,$$

consistent with R = 1.6. In the most acidic (pH = 1.5) conditions, SO_2 formation is expected as an intermediate step in the oxidation of $S_4O_6^{2-}$ to SO_4^{2-}. Degassing of $SO_{2(g)}$ would result in $R < 1.6$, again consistent with experimental observations. The above multistep mechanism, based on known aqueous redox chemistry of sulfur species, accounts for the deficit in aqueous sulfur noticed in all published experimental observations. The intermediate species cannot be detected, and it is consistent with calculated concentrations being below the detection limits. Under nonacidic conditions, $S_2O_3^{2-}$ can be detected, but evaluation of the dissolution mechanism is hindered by precipitation of Fe(III) as iron oxyhydroxides. *Copyright © 2004 Elsevier Ltd*

1. INTRODUCTION

Pyrite (FeS_2) is one of the major minerals on Earth, participating in the sulfur and iron global cycles. Pyrite is known as a redox buffer in anoxic conditions (Beaucaire et al., 2000), and therefore as a redox sink for sulfur and iron, since its solubility is very low (Berner, 1984). Its presence, synonymous of reducing conditions, is used as an indicator for uranium and other metal hydrothermal ores in geochemical exploration (Rich et al., 1977). The surface reactivity of pyrite is often discussed in the context of the origin of life (McClendon, 1999; Wächtershäuser, 2000), sorption of precious metals such as Au and Ag (Scaini et al., 1997), and pyrite is also mentioned in relation to solar energy devices (Ennaoui et al., 1986). Finally, pyrite oxidation by oxygen or another oxidant, according to

$$FeS_2 + 7/2O_2 + H_2O \rightarrow Fe^{2+} + 2SO_4^{2-} + 2H^+ \quad (1)$$

leads to the release of two moles of H^+ per mole of oxidized pyrite. Acidification can be further enhanced by the oxidation of iron according to

$$FeS_2 + 15/4O_2 + 7/2H_2O \rightarrow Fe(OH)_{3(s)} + 2SO_4^{2-} + 4H^+, \quad (2)$$

and ferric iron, produced in reaction 2, is also known as a strong oxidant of pyrite in strongly acidic conditions (Garrels and Thomson, 1960; Singer and Stumm, 1970; Moses et al., 1987). This oxidation autocatalysis can be written

$$FeS_2 + 14Fe^{3+} + 8H_2O \rightarrow 15Fe^{2+} + 2SO_4^{2-} + 16H^+. \quad (3)$$

Reactions (1–3) described processes producing acid mine

* Author to whom correspondence should be addressed (michael.descostes@cea.fr).
† Present address: IRSN/DPRE/SERGD, F-92265 Fontenay-aux-Roses, France

Table 1. Details of dissolution experiment conditions.

Run	Media	Duration (min)
M02	$HClO_4$ 10^{-2} mol L^{-1}	294
M04	$HClO_4$ 10^{-2} mol L^{-1}	369
M05	$HClO_4$ 10^{-3} mol L^{-1}	471
M07	$HClO_4$ 10^{-2} mol L^{-1}	261
M10	$HClO_4$ 10^{-2} mol L^{-1}	361
M12	$HClO_4$ 10^{-2} mol L^{-1}	406
M13	HCl 10^{-2} mol L^{-1}	365
M19	$HClO_4$ 10^{-3} mol L^{-1}	360
M21	HCl $10^{-1.5}$ mol L^{-1}	360
M22	$HClO_4$ 10^{-2} mol L^{-1}	1507

drainage, well documented down stream from sulfide ore mining (see, for example, the Doñana ecological disaster in Spain: Pain et al., 1998 or Evangelou, 1995).

FeS_2 oxidative dissolution has been studied using most techniques available, including electrochemistry (Bailey and Peters, 1976; Biegler and Swift, 1979; Wei and Osseo-Asare, 1997), solution chemistry (McKibben and Barnes, 1986; Nicholson et al., 1988, 1990; Kamei and Ohmoto, 2000), spectroscopic and other techniques (Taylor et al., 1984; Fornasiero et al., 1992; Donato et al., 1993; Knipe et al., 1995; Descostes et al., 2001, 2002; McGuirre et al., 2001). Recently, synchrotron X-ray photon electron spectroscopy surface (Guevremont et al., 1998; Schaufus et al., 1998; Nesbitt et al., 2000; Uhlig et al., 2001) and scanning tunnelling microscopy under ultra-high vacuum (Rosso et al., 1999a,b) have been used to investigate the pyrite surface at an atomic scale. Despite all these efforts, no consensus has yet emerged on a single and well-established oxidation mechanism.

Recent literature focuses on acidic dissolution observed by spectroscopic techniques. Sasaki et al. (1995) observed a sulfur-rich layer on a pyrite surface oxidized in ferric medium ($FeCl_3 \cdot 6H_2O$ 15 mmol L^{-1}) at pH = 2 over 72 h. These authors proposed nonstoichiometric oxidation of pyrite, with preferential dissolution of iron, as also proposed by several other authors (Buckley and Woods, 1987; Mycroft et al., 1990; Zhu et al., 1994; Ahlberg and Broo, 1997; Bonnissel-Gissinger et al., 1998; Toniazzo et al., 1999; McGuirre et al., 2001). Nevertheless, Luther (1997) argued against this interpretation (see also Sasaki et al., 1997), based on his mechanism proposed earlier from electronic orbital considerations (Luther, 1987) and sulfur aqueous chemistry. Luther (1997) proposed that the sulfur-rich layer on the pyrite surface is not a direct oxidation product, but arises from the disproportion of thiosulfate ($S_2O_3^{2-}$), the actual oxidation product of pyrite, into elementary sulfur (S_8 or S^0) and bisulfite (HSO_3^-) according to:

$$8S_2O_3^{2-} + 8H^+ \rightarrow S_8 + 8HSO_3^- \quad (4)$$

The sulfur enrichment of the oxidized pyrite surface analysed by Sasaki et al. (1995) would then result, not from nonstoichiometric dissolution with preferential iron removal, but from

Table 2. Analytical results for experiments in $[HClO_4] = 10^{-2}$ mol L^{-1} medium.

Run	Medium	Time min	[Fe] μmol L^{-1}	σ	$Fe^{(II)}$ %	σ	$Fe^{(III)}$ %	σ	$[SO_4^{2-}]$ μmol L^{-1}	σ	R	σ	pH	Eh mV/ESH
M04	$[HClO_4] = 10^{-2}$ mol L^{-1}	—	0	0	—	—	—	—	0	0	—	—	2.089	732.5
		5	6.5	0.7	79.7	4.0	20.3	1.0	12	1	1.8	0.3	2.092	667.2
		21	9.9	0.7	72	4	28	1	18	1	1.8	0.2	2.107	667.5
		33	12.6	0.7	94	5	6.2	0.3	19	2	1.5	0.2	2.114	662.8
		43	16.6	0.8	89	4	10.8	0.5	16	1	0.96	0.08	2.116	664.8
		66	17.5	0.8	85	4	14.9	0.7	20.5	0.8	1.171	0.070	2.121	665.2
		128	19.3	0.8	93	5	7.1	0.4	24	3	1.2	0.2	2.114	668.5
		166	15.3	0.8	78	4	21.7	1.1	22	1	1.438	0.100	2.114	670.3
		216	20.4	0.7	98	5	2.1	0.1	28	1	1.37	0.07	2.102	672.8
		281	21.0	1.0	80.5	4.0	19.5	1.0	31	3	1.5	0.2	2.107	675.2
		369	22.0	0.9	89	4	11.5	0.6	94	2	4.27	0.20	2.099	—
M07	$[HClO_4] = 10^{-2}$ mol L^{-1}	0	0	0	—	—	—	—	0	0	—	—	2.032	762.5
		5	2.3	0.3	—	—	—	—	3.5	0.3	1.5	0.3	2.042	705
		25	4.3	0.6	—	—	—	—	5.7	0.4	1.3	0.2	2.057	691.1
		46.5	4.2	0.6	—	—	—	—	6.5	0.3	1.5	0.2	2.05	685.5
		93	4.5	0.7	—	—	—	—	8.2	0.3	1.8	0.3	2.045	671.1
		189	5.8	0.9	—	—	—	—	9.0	0.4	1.5	0.2	2.049	655.3
		261	6.4	1.0	—	—	—	—	9.0	0.4	1.4	0.2	2.050	644.9
M10	$[HClO_4] = 10^{-2}$ mol L^{-1}	0	0	0	—	—	—	—	0	0	—	—	2.041	726.0
		5	2.1	0.3	79	4	22	1	5.1	0.5	2.4	0.4	2.044	674.8
		22	4.1	0.6	95	5	5.0	0.3	12.4	0.5	3.0	0.5	2.044	670.6
		42	3.5	0.5	87	4	12.7	0.6	16.0	0.5	4.5	0.7	2.046	664.7
		62	5.0	0.7	86	4	13.8	0.7	18.5	0.6	3.7	0.6	2.046	660.8
		93	6.1	0.9	79	4	21	1	21.4	1.0	3.5	0.6	2.046	658.3
		214	9	1	93	5	6.8	0.3	24.3	0.8	2.7	0.4	2.049	649.9
		333	11	2	85	4	15.0	0.8	27	2	2.4	0.4	2.053	642.9
		361	12	2	87	4	12.7	0.6	25	1	2.1	0.3	2.054	—
M22	$[HClO_4] = 10^{-2}$ mol L^{-1}	0	0	0	—	—	—	—	0	0	—	—	—	—
		360	10	2	—	—	—	—	16.1	0.9	1.5	0.2	—	—
		727	17	3	—	—	—	—	21	1	1.2	0.2	—	—
		1507	26	4	—	—	—	—	34	2	1.3	0.2	—	—

Table 3. Analytical results for experiments in [HCl] = $10^{-1.5}$ and 10^{-2} mol L^{-1} and [$HClO_4$] = 10^{-3} mol L^{-1} media.

Run	Medium	Time min	[Fe] μmol L^{-1}	σ	$Fe^{(II)}$ (%)	σ	$Fe^{(III)}$ (%)	σ	$[SO_4^{2-}]$ μmol L^{-1}	σ	R	σ	pH	Eh mV/ESH
M05	[$HClO_4$] = 10^{-3} mol L^{-1}	0	0	0	—	—	—	—	0	0	—	—	2.998	644.4
		5	0.5	0.2	54	3	46	2	13	2	26	11	3.025	628.3
		27	1.5	0.1	100	5	0	0	20.9	0.8	14	1	3.112	601.4
		52	1.9	0.1	100	5	0	0	27.5	1	14.5	0.9	3.091	593.3
		72	2.39	0.07	79.97	4.00	20.03	1.00	18.4	0.7	7.7	0.4	3.077	591.1
		94	2.6	0.1	100	5	0	0	37.3	0.9	14.3	0.7	3.062	590.5
		124	3	0.2	100	5	0	0	51	2	17.0	1.3	3.037	590.6
		169	3.4	0.2	82.6	4.1	17.4	0.9	53	2	16	1	3.045	—
		231	3.6	0.1	75	4	25	1	57	5	16	1	—	—
		298	4.2	0.1	81.4	4.1	18.7	0.9	68	1	16.2	0.5	—	—
		357	4.7	0.2	76	4	24	1	69	1	14.7	0.7	—	606.7
		471	5.5	0.3	88.7	4.4	11.3	0.6	85	2	15.5	0.9	—	600.9
M13	[HCl] = 10^{-2} mol L^{-1}	0	0	0	—	—	—	—	0	0	—	—	2.014	673.2
		5	1.9	0.3	—	—	—	—	8	1	4	0.8	2.012	629.2
		20	4.6	0.7	—	—	—	—	11	2	2.4	0.5	2.002	641.7
		40	4.9	0.7	—	—	—	—	12	2	2.3	0.6	2.004	645.8
		60	5.2	0.8	—	—	—	—	11.5	1.0	2.2	0.4	2.006	648.5
		90	6.4	1.0	—	—	—	—	13	1	2.0	0.3	2.007	645.1
		150	7	1	—	—	—	—	13	1	1.763	0.300	2.009	638.6
		180	8	1	—	—	—	—	13.4	1.0	1.6	0.3	2.011	638.0
		270	9	1	—	—	—	—	13	1	1.5	0.3	2.014	638.2
		365	10	2	—	—	—	—	16.3	1.0	1.6	0.3	2.016	639.0
M19	[$HClO_4$] = 10^{-3} mol L^{-1}	0	0	0	—	—	—	—	0	0	—	—	3.057	676.9
		5	1.5	0.2	—	—	—	—	7	2	4	1	3.062	639.8
		20	2.3	0.3	—	—	—	—	7	2	3.3	0.9	3.052	632.0
		40	3.5	0.5	—	—	—	—	8	2	2.4	0.6	3.068	626.5
		60	3.7	0.6	—	—	—	—	9	2	2.4	0.6	3.083	626.4
		90	5.2	0.8	—	—	—	—	10	2	2.0	0.4	3.080	627.4
		180	6.69	1.00	—	—	—	—	11	2	1.7	0.3	3.090	622.3
		274	8	1	—	—	—	—	12	2	1.48	0.30	3.089	616.1
		360	9	1	—	—	—	—	12	2	1.3	0.3	3.094	612.4
M21	[HCl] = $10^{-1.5}$ mol L^{-1}	0	0	0	—	—	—	—	0	0	—	—	1.577	736.6
		5	4.6	0.5	1.9	0.1	98	5	6	2	1.2	0.4	1.575	670.0
		20	6.2	0.6	22	1	78	4	8	2	1.3	0.3	1.579	659.7
		40	6.7	0.7	8.5	0.4	91	5	8	2	1.1	0.3	1.583	655.6
		60	7.7	0.8	0	0	100	5	8	2	1.1	0.3	1.592	653.1
		90	7.8	0.8	1.8	0.1	98	5	13	2	1.7	0.3	1.600	651.6
		120	7.7	0.8	2.0	0.1	98	5	9.7	2.0	1.3	0.3	1.606	650.2
		180	8.7	0.9	0.0	0	100	5	12	2	1.4	0.3	1.631	647.0
		270	9.5	0.9	9.9	0.5	90	5	10	2	1.1	0.2	1.644	640.9
		360	9.8	1.0	15.7	0.8	84	4	11.8	2.0	1.2	0.2	1.665	637.3

precipitation of elementary sulfur (see also Rimstidt and Vaughan, 2003). To resolve this issue, both pyrite surface chemistry and aqueous chemistry of iron and sulfur have to be taken into account to thoroughly interpret any experimental data on pyrite oxidation.

Few studies have focused on aqueous sulfur chemistry (Steger and Desjardins, 1978; Goldhaber, 1983; Schippers et al., 1999 in the case of bioleaching), probably because of analytical difficulties. Yet, ignoring the aqueous chemistry can result in biased conclusions when describing nonstoichiometric dissolution processes. Basolo and Pearson (1958) concluded that any elementary redox reaction is certainly limited to a maximum of two electrons net transfer. Therefore, pyrite oxidation is expected to result in the production of several intermediate sulfoxyanion species with increasing oxidation numbers from (−I), as in FeS_2, to (+VI), as in SO_4^{2-}.

Williamson and Rimstidt (1994) have compiled data from different studies and hence proposed kinetic laws for pyrite oxidation as functions of O_2, Fe(III) and both oxidants. However, this comparison is difficult, since experimental conditions from one study to another (such as water/solid ratio, solid preparation methods, etc.) are very different. To overcome this problem, Ichikuni (1960) focused on the ratio $R = [S]_{tot}/[Fe]_{tot}$ to interpret his experimental data for the dissolution of pyrite in aqueous solutions at pH values ranging from 1.1 to 3.2. A value of $R = 2$ corresponds to a stochiometric dissolution. Although the parameter R can be used to directly compare dissolution experiments under different chemical and physical conditions, there is no other use made of this experimental parameter, to our knowledge. We decided to use a similar treatment of experimental data, i.e., using the $R = [S]_{tot}/[Fe]_{tot}$ aqueous ratio measured in batch dissolution experiments at pH $\cong$ 2, in addition to solid characterization methods. Pyrite surfaces free of any oxidation products were dissolved in acidic media to avoid iron hydrolysis and precipitation, and sulfur and iron aqueous speciation was monitored. With these controlled chemical conditions, we were able to verify experimentally the hypothesis of Luther (1987, 1997).

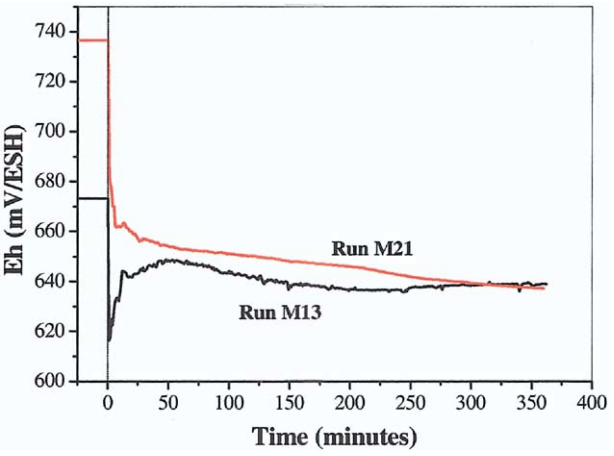

Fig. 1. Comparison of redox potential (Eh) trends in [HCl] = 10^{-2} mol L^{-1} (run M13) and [HCl] = $10^{-1.5}$ mol L^{-1} (run M21) media.

2. MATERIALS AND METHODS

2.1. Sample Characterisation and Preparation

Pyrite samples were obtained from Spain (Logroño). All pyrite crystals were about a centimeter across and as cubes. No chemical zoning was observed. Samples of pyrite were first dipped in 37% HCl for several hours to remove any oxidation products present at the mineral surface. The pyrite was then introduced into a glove box with partial pressures of H_2O ($p(H_2O)$) and O_2 ($p(O_2)$) both below 1 ppm and rinsed with acetone. The mineral was ground in an agate mortar and sieved with ethanol (grain sizes in the 150–250 μm fraction being selected). Pyrite was then washed in ultra-sonic bath to remove any fine particles adhering to the grain surfaces. These two operations were repeated until the ethanol after the ultrasonic-bath treatment was clear, and free of fine particles, as checked by scanning electron microscopy (SEM). Samples were kept in a glove box until the experiments. Surface purity was controlled by X-ray photoelectron spectroscopy (XPS) showing no oxidation products. Chemical analysis was performed by SEM-based energy dispersive X-ray spectroscopy, with over 40 points per sample analysed showing the stoichiometric ratio expected for pyrite (S/Fe = 1.99 ± 0.03). Some samples were analyzed to determine chemical impurities (Zn, Cu, Mn, Co, Cr, Ni, As, Ag, Mo, Pb, Hg and Se). Chemical analyses of FeS_2 were performed at CNRS-CRPG (see Acknowledgments). Sample characterization by X-ray diffraction (XRD) was also used to confirm the absence of any accessory minerals. The protocol of sample preparation was also controlled by other techniques, such as BET, sample dissolution experiments (Descostes, 2001) and additional solid characterization by XPS and nuclear microprobe (Descostes et al., 2001). N_2-BET (0.028 ± 0.003 $m^2 \cdot g^{-1}$), Ar-BET (0.031 $m^2 \cdot g^{-1}$) and Kr-BET (0.036 ± 0.004 $m^2 \cdot g^{-1}$) gave consistent results for surface area. Before analysis by XPS, powder samples were pressed into an indium foil of ~1 cm^2 surface area. The quantity of powder used for this preparation was chosen so that the indium foil was completely covered by the product. XPS analyses were carried out using a VG Escalab MKII spectrometer with unmonochromated AlK_α (1486.6 eV) radiation. The experimental conditions were a source power of 10 kV and 5 mA with the analysis chamber pressure lower than 10^{-8} Pa. Detection limits were estimated as between 1 and 0.1 atomic percent (see Descostes et al., 2000, for more details).

2.2. Dissolution Experiments

All solutions used in this study were made with ultrapure deionized water (18.2 MΩ cm^{-1}). Commercial salts and acid used were all of American Chemical Society (ACS) reagent grade or higher quality and purity. Batch experiments were run in glass electrochemistry cells, thermostated at 25.0 ± 0.1°C in contact with air. Agitation was performed by a magnetic stirrer guaranteeing a continuously homogeneous solution. The water to solid ratio was 150 mL g^{-1}. Dissolution experiments were carried out in HCl and $HClO_4$ media at pH values around 2 and 3 (Merck Titrisol 109970 and Prolabo Titrinorm 30111.291). Two different contact times of ~6 h and ~24 h were selected to discriminate a hypothetical transient state from a stationary one. All experiments are detailed in Table 1. Aliquots were sampled using a prefilter (Interchim CH821770), then filtered at 0.22 μm (Nalgene 190-2520) and immediately analysed for sulfur and iron. The number of samples was limited to keep variations of the solid-solution ratio to < 10% of the initial value. The final solid samples were kept in anoxic glove box before XPS analysis.

2.3. Analysis in Solutions

Sulfur aqueous speciation and analysis were performed by both ionic chromatography (Dionex analyser DX4500 using an IonPac AS14 analytical column and AG14 guard column in $[Na_2CO_3]$ = 3.5 mmol L^{-1} + $[NaHCO_3]$ = 1 mmol L^{-1} eluent) and capillary electrophoresis (Waters Quanta 4000), following protocols detailed in Motellier et al. (1997) and Motellier and Descostes (2001). $[Fe]_{tot}$ were determined by furnace atomic absorption spectrometry (UNICAM 939, λ = 248.3 nm). Oxidation state of iron was investigated by spectrophotometry (Viollier et al., 2000). Electrochemical parameters (pH and Eh) were followed after calibration (5 pH buffers and 1 Eh buffer) with a pH glass electrode (Radiometer XG250) and a Pt electrode (Radiometer XR110) each coupled with a calomel reference electrode (Radiometer REF451) connected to an ionometer (Radiometer PHM250). Data were collected and recorded on an informatic interface.

3. RESULTS AND INTERPRETATION

Tables 2 and 3 show all of the results. Only marginal variations of pH were observed during the dissolution duration, whatever the experiment. The pH remaining fairly constant can be easily understood, as the maximum number of protons released upon dissolution (i.e., 2 × $[Fe]_{tot}$ = 50 μmol L^{-1}) is negligible compared to $[H^+]_{init} \geq 10^{-3}$ M.

Eh initially dropped dramatically upon mineral introduction, and then increased with time, following the same trend as pH (Fig. 1). The initial decrease in Eh can be easily understood, since Eh is not initially buffered by redox-active species, while the dissolution of pyrite will produce iron and sulfur, known for their electroactive behavior. Calculations indicate that the Eh values measured are consistent with the Eh values imposed by Fe^{3+}/Fe^{2+} couple.

Trends of $[SO_4^{2-}]$ and $[Fe]_{tot}$ as a function of time are different from one run to another for the same medium, indicating different dissolution rates (Figs. 2 and 3). Let us consider the $[HClO_4] = 10^{-2}$ mol L^{-1} medium as an example: $[SO_4^{2-}]$ and $[Fe]_{tot}$ in runs M07, M10 and M22 are lower than in M04. At 360 min, $[Fe]_{tot}$ in runs M10 and M22 are respectively equal to 12 and 10 μmol L^{-1}, but nearly twice as great (22 μmol L^{-1}) in run M04. Dissolved iron is mainly divalent (up to 95% of $[Fe]_{tot}$) except for run M21 where Fe^{3+} predominates. Dissolved sulfur is exclusively as the SO_4^{2-} form. No dissolved sulfoxyanion was detected. Furthermore, oxidation of samples by H_2O_2 did not show any difference between $[S]_{tot}$ and $[SO_4^{2-}]$. Cruz et al. (2001) showed that other metal sulfides in contact of pyrite induce a surface passivation, thereby strongly altering surface reactivity and reducing the dissolution rate. Indeed, in our dissolution experiments, we observed a great disparity with time in rates of $[SO_4^{2-}]$ and $[Fe]_{tot}$. The disparity can be traced to the presence of chemical impurities in our natural pyrite samples, since analysis typically showed significant As in one set of samples, whereas it was not detected in

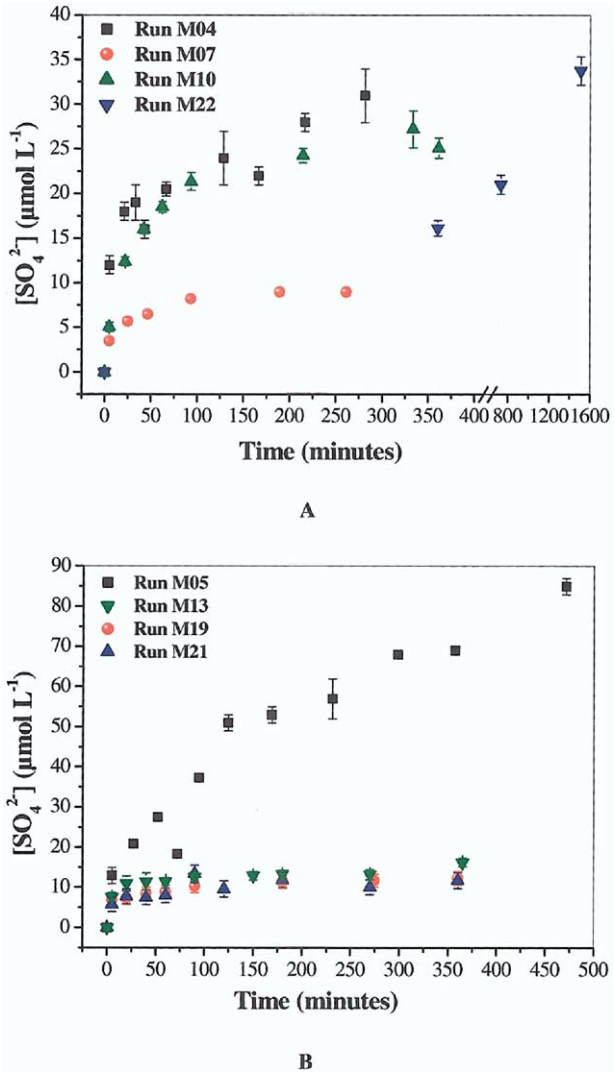

Fig. 2. Comparison of sulfate content trends (A) $[HClO_4] = 10^{-2}$ mol L^{-1}— runs M04, M07, M10 and M22. (B) $[HCl] = 10^{-1.5}$ mol L^{-1}— run M21, $[HCl] = 10^{-2}$ mol L^{-1}— run M13 $[HClO_4] = 10^{-3}$ mol L^{-1}— runs M05 and M19.

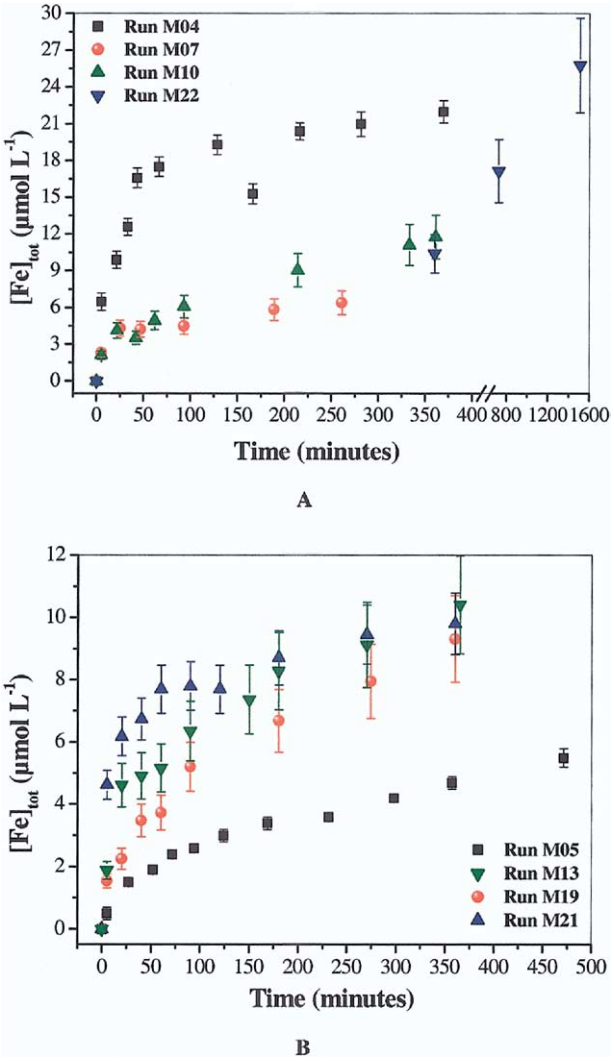

Fig. 3. Comparison of iron content trends (A) $[HClO_4] = 10^{-2}$ mol L^{-1}— runs M04, M07, M10 and M22. (B) $[HCl] = 10^{-1.5}$ mol L^{-1}—run M21, $[HCl] = 10^{-2}$ mol L^{-1}— run M13 $[HClO_4] = 10^{-3}$ mol L^{-1}— runs M05 and M19.

the other samples, that also contain higher Co and Ni contents (Table 4). Therefore, release rates are not reliable parameters to use to establish a reaction mechanism of pyrite dissolution.

Whatever the variations of $[Fe]_{tot}$ and $[SO_4^{2-}]$, R ratios ($=[SO_4^{2-}]/[Fe]_{tot}$, as $[S]_{tot} = [SO_4^{2-}]$) eventually converge toward a value of R = 1.6, except for run M05 (Fig. 4). Furthermore, the dispersion in R values is smaller than in $[Fe]_{tot}$ and $[SO_4^{2-}]$. R seems therefore a more appropriate experimental parameter. R varies as a function of time, over two distinct intervals. In the first interval, $R > 2$. This period either can be very short, lasting less than 60 min in run M04, or can extend over the whole run duration, as for run M10 (Fig. 4). Over this transient time interval, R values are not reproducible from experiment to experiment. This period presumably corresponds to a first stage of pyrite dissolution. The second time interval is characterized by $R < 2$, usually close to 1.60, but down to 1.25 for run M21. Such R values are also observed for long duration experiments (see, for example, run M22, 1500 min) and may point to a permanent dissolution regime. Only experiment M05 is inconsistent, with an R value close to 15 whatever the run duration. We will only focus on the second time interval, because the R values are generally reproducible and are assumed to originate from a permanent dissolution regime.

Through Eh conditions, iron is generally in the form of Fe^{2+} or Fe^{3+} and $[Fe]_{tot}$ values are below the solubility limits of all known ferric hydroxide or oxy-hydroxide minerals in the pH ranges of most of the experiments, except for run M05. In the M05 case, an R value close to 15, coupled with an increase in pH, can be explained by precipitation of a ferric hydroxide compound. In the other dissolution experiments, after a brief increase at the beginning of the experiment, the pH decreased slightly from 3.12 to 3.00, a value close to the initial pH (Fig. 5). This variation can be originated in acidification produced by both pyrite dissolution and precipitation of ferric hydroxide or

Table 4. Chemical composition of pyrite samples used in this study (Fe and S in wt%; Zn, Cu, Mn, Co, Cr, Ni, Pb, Ag, As, Mo, and Se in ppm; Hg in ppb).

Sample	Fe	S	Zn	Cu	Mn	Co	Cr	Ni	Pb	Ag	As	Mo	Se	Hg
1	45.59	52.67	12	5	8	27	<10	<10	0.7	<0.1	93	<0.4	4.5	24
2	45.91	53.85	12	7	7	22	<10	<10	1.3	<0.1	104	<0.4	5.2	20
3	43.96	50.17	35	12	66	816	32	672	13.7	0.17	1.5	<0.4	10.8	96
4	44.75	51.17	20	6	51	254	24	876	8.7	0.16	1.1	<0.4	5.2	22
5	44.82	51.65	25	9	25	363	21	762	11.9	0.15	1.2	<0.4	11.2	54
6	44.72	51.41	20	7	48	187	28	583	7.1	0.15	3.1	<0.4	5.8	33

oxy-hydroxide ($Fe(OH)_3$ or FeOOH) (Reaction 2) if H^+ produced by pyrite dissolution is estimated from the sulfate content (i.e., 170 μmol L^{-1}).

4. DISCUSSION

4.1. Comparison with Previous Work

To achieve consistency and determine a plausible mechanism of pyrite dissolution in acidic media, it is desirable to discuss our results alongside those of previously published studies of pyrite dissolution. However, most pyrite oxidation studies do not provide values of dissolved concentrations of iron and sulfur, not to mention R ratios. Only the work of Ichikuni (1960), McKibben and Barnes (1986) and Bonnissel-Gissinger et al. (1998) could be used to estimate R values. Data gathered in Table 5 are extrapolated from kinetic curves published by these authors.

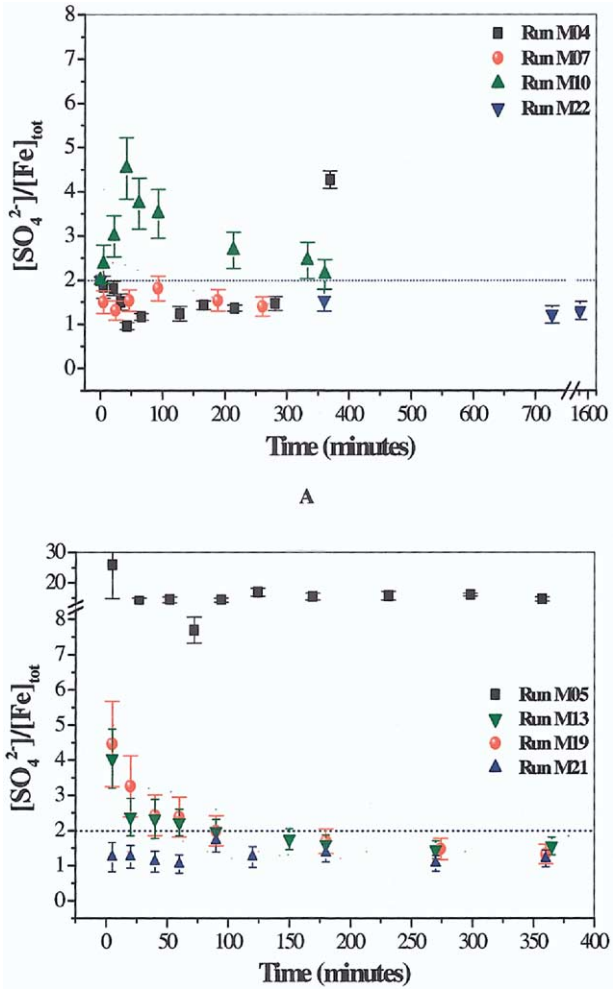

Fig. 4. Comparison of $R = [SO_4^{2-}]/[Fe]_{tot}$ trends (A) $[HClO_4] = 10^{-2}$ mol L^{-1}— runs M04, M07, M10 and M22. (B) $[HCl] = 10^{-1.5}$ mol L^{-1}— run M21, $[HCl] = 10^{-2}$ mol L^{-1}— run M13 $[HClO_4] = 10^{-3}$ mol L^{-1}— runs M05 and M19.

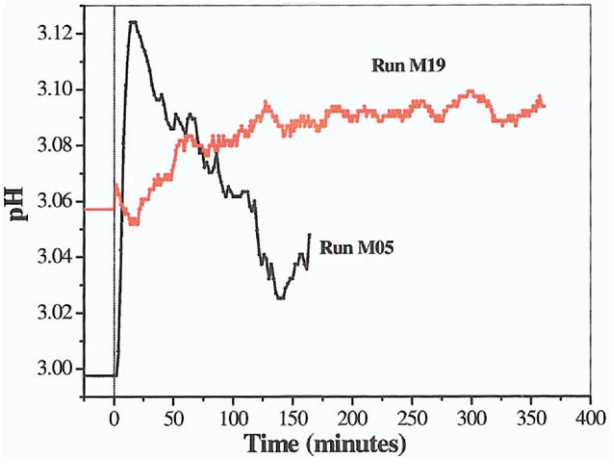

Fig. 5. Comparison of pH trends in $[HClO_4] = 10^{-3}$ mol L^{-1} medium (runs M05 and M19).

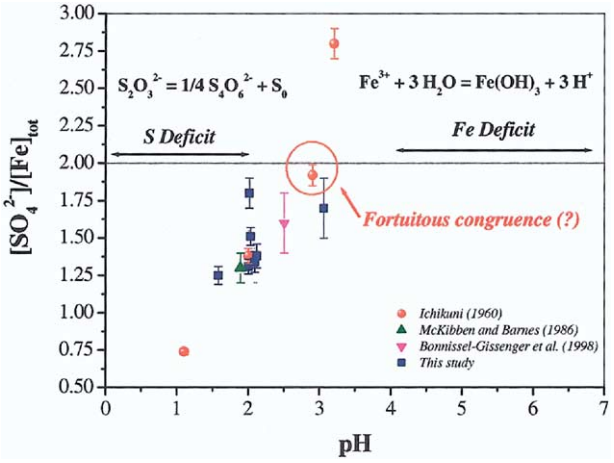

Fig. 6. Comparison of $R = [SO_4^{2-}]/[Fe]_{tot}$ calculated in this study and from data taken from the literature.

Table 5. Ratios R = $[SO_4^{2-}]/[Fe]_{tot}$ calculated from data taken from Ichikuni (1960), McKibben and Barnes (1986), and Bonnissel-Gissinger et al. (1998).

pH	Medium	R announced	R calculated	Reference
1.1	HCl 10^{-1} mol L^{-1}	0.67	0.74 ± 0.02	Ichikuni (1960)
1.89	HCl + H_2O_2	—	1.3 ± 0.1	McKibben and Barnes (1986)
2	HCl 10^{-2} mol L^{-1}	1.57	1.38 ± 0.05	Ichikuni (1960)
2.5	HNO_3	—	1.6 ± 0.2	Bonnissel-Gissinger et al. (1998)
2.9	HCl 10^{-3} mol L^{-1}	2.7	1.92 ± 0.07	Ichikuni (1960)
3.2	H_2O	4.78	2.8 ± 0.1	Ichikuni (1960)

Ichikuni (1960) studied pyrite oxidation in [HCl] = 10^{-1} mol L^{-1} (pH = 1.89), [HCl] = 10^{-2} mol L^{-1} (pH = 2.0), [HCl] = 10^{-3} mol L^{-1} (pH = 2.9) and H_2O (pH = 3.2) in contact with the atmosphere at 80°C. This author calculated $[SO_4^{2-}]/[Fe]_{tot}$ from iron and sulfate production rates. We have recalculated ratios from $[SO_4^{2-}]$ and $[Fe]_{tot}$. Values diminish with the pH of the reaction medium, from R = 0.74 ± 0.02, to R = 1.38 ± 0.05, R = 1.92 ± 0.07 and R = 2.8 ± 0.1, for [HCl] = $10^{-1.5}$, 10^{-2}, 10^{-3} mol L^{-1} and H_2O media, respectively. R > 2 measured in a dilute medium (H_2O) reveals a deficit in aqueous iron, as in our M05 experiment. Moderate pH favors iron hydrolysis and precipitation as seen in Descostes et al. (2002). McKibben and Barnes (1986) studied pyrite oxidation in chloride medium at pH = 1.89, in contact with the atmosphere and H_2O_2 ($[H_2O_2]$ = 144 μmol L^{-1}) at 30°C. In these experiments, R is always lower than 2, and the mean calculated R value equals 1.3 ± 0.1. Bonnissel-Gissinger et al. (1998) have carried out pyrite dissolution experiments in oxidizing conditions at several pH values, notably at pH = 2.5 in HNO_3 medium at 25°C. The calculated R ratio for their experiments equals R = 1.6 ± 0.2 after 36 h of dissolution.

When R ratios obtained in this study are compared to those from the literature, three pH fields can be distinguished (Fig. 6). Firstly, R < 2 occurs in very acidic to moderately acidic media (pH ≤ 2). Results from our study are in good agreement with those from McKibben and Barnes (1986), Ichikuni (1960) and Bonnissel-Gissinger et al. (1998). We will discuss this point in the next section. Secondly, at pH = 3, R = 2 (maybe fortuitously), which is in agreement with the solid stoichiometry ratio of pyrite. Thirdly, at pH > 3, R > 2, as a result of iron precipitation by hydrolysis.

4.2. Reaction Mechanism at pH < 3

Nonstoichiometric dissolution with R < 2 can result either from an excess release of iron, leaving a sulfur-enriched layer at the pyrite surface, or from pyrite congruent dissolution followed by removal of dissolved sulfur species. The comparisons between the different sets of experiments show that $[Fe]_{tot}$ are comparable for similar reaction periods, while $[SO_4^{2-}]$ can reach very low values in run M21 ([HCl] = $10^{-1.5}$ mol L^{-1}). In this last case, R = 1.25 is the lowest value recorded for all experiments, likely indicating a deficit in aqueous sulfur. Therefore, pyrite dissolution in acidic media has the appearance of being incongruent.

Sulfur deficit at pH < 3 cannot reasonably be explained by precipitation of any known ferric or ferrous salt, since in these conditions, the saturation indices are lower than 1. We have already seen that ferric iron can be reduced by pyrite in an acidic medium (Singer and Stumm, 1970) according to reaction 3. However, this would result in R = 0.133, well below our experimental values.

The only possible explanation for the observed nonstoichiometry in pyrite dissolution is that sulfur is removed from the solution, either as a solid, or as a gas. In both cases, this removal indicates that sulfur species other than S_2^{2-} and SO_4^{2-}, the stable sulfur species, are present in the solution. Such species could be one of the products of an intermediate disproportionation step, while the other product(s) of the disproportionation would be soluble and further oxidized to S(VI). Metastable sulfur species must form upon FeS_2 oxidation, and consequently the oxidation of pyrite into Fe^{2+} and SO_4^{2-} cannot be described by a single elementary step. In the first step, pyrite dissolves, with release of an aqueous sulfur species $S^{(n)}$ ($0 < n < 6$) according to

$$FeS_2 \rightarrow Fe^{2+} + 2\,S^{(n)} + 2\,(n+1)e^-. \quad (5)$$

$S^{(n)}$ species should then disproportionate into another sulfur species $S^{(n')}$ with an oxidation number n' ($n' > n$), and metastable S^0 (which would not be oxidized for thermodynamic or kinetic reasons) according to the reaction:

$$S^{(n)} \rightarrow \frac{n}{n'}\,S^{(n')} + \frac{n'-n}{n'}S^0 \quad (6)$$

Finally, $S^{(n')}$ species would be oxidized into SO_4^{2-} in a third stage:

$$S^{(n')} \rightarrow S^{(VI)} + (6-n')e^-. \quad (7)$$

Mass balance of Reaction 7 is

$$[SO_4^{2-}] = [S^{(VI)}] = [S^{(n')}]. \quad (8)$$

Mass balance of reaction 6 is

$$[S^{(n)}] = \frac{n'}{n}[S^{(n')}] = \frac{n'}{n}[SO_4^{2-}], \quad (9)$$

where Eqn. 8 is taken into the right-hand side of Eqn. 9. Mass balance for reaction 5 is

$$\left[Fe\right]_{total} = \left[Fe^{2+}\right] = 0.5\left[S^{(n)}\right] = 0.5\,\frac{n'}{n}\left[SO_4^{2-}\right], \quad (10)$$

where Eqn. 9 is taken into the right-hand side of Eqn. 10. Finally, from Eqn. 10, R = $[SO_4^{2-}]/[Fe]_{tot}$ can be easily expressed as

Table 6. Ratios $[SO_4^{2-}]/[Fe]_{tot}$ (R) less than or equal to 2 in function of $S^{(n)}$ and $S^{(n')}$ ($0 < n < n'$ and $n' \leq 6$) inherited from the pyrite oxidation with a disproportion step into S^0; ΔG_R of the disproportion step is also indicated (in kJ mol^{-1}). See Descostes (2001) for thermodynamic data.

$S^{(n)}$	n	$S^{(n')}$	n'	ΔG_R	R
$S_2O_3^{2-}$	2	$S_4O_6^{2-}$	2.5	−36.0	1.60
		$S_3O_6^{2-}$	10/3	−3.1	1.20
		SO_2	4	−14.9	1.00
		$S_2O_6^{2-}$	5	−6.4	0.8
		SO_4^{2-}	6	−58.8	0.67
$S_5O_6^{2-}$	2	$S_4O_6^{2-}$	2.5	−82.4	1.60
		$S_3O_6^{2-}$	10/3	0.0	1.20
		SO_2	4	−29.6	1.00
		$S_2O_6^{2-}$	5	−8.4	0.8
		SO_4^{2-}	6	−124.3	0.67
$S_4O_6^{2-}$	2.5	SO_4^{2-}	6	−41.9	0.83
$S_2O_4^{2-}$	3	$S_3O_6^{2-}$	10/3	−70.2	1.8
		SO_3^{2-}	4	−11.6	1.5
		SO_2	4	−88.0	1.5
		$S_2O_5^{2-}$	4	−52.8	1.5
		$S_2O_6^{2-}$	5	−75.2	1.2
		SO_4^{2-}	6	−144.7	1
$S_3O_6^{2-}$	10/3	SO_2	4	−29.6	1.67
		$S_2O_6^{2-}$	5	−8.4	1.33
		SO_4^{2-}	6	−124.3	1.11
SO_2	4	$S_2O_6^{2-}$	5	−42.4	1.6
		SO_4^{2-}	6	−88.7	1.33
SO_3^{2-}	4	SO_4^{2-}	6	−37.9	1.33
$S_2O_5^{2-}$	4	$S_2O_6^{2-}$	5	−29.9	1.60
		SO_4^{2-}	6	−122.6	1.33
$S_2O_6^{2-}$	5	SO_4^{2-}	6	−115.9	1.67

$$R = \frac{2n}{n'} \quad (11)$$

with $0 < n < n' \leq 6$. The net oxidation reaction is obtained by combining reactions 6 and 7 into reaction 5, consistent with Eqn. 11:

$$FeS_2 \rightarrow Fe^{2+} + 2\left[1 + \frac{6n}{n'}\right]e^- + \frac{2n}{n'}S^{VI} + 2\ \frac{n'-n}{n'}S^0 \quad (12)$$

The symbol $S^{(n)}$ refers to the species $S_xO_y^{z-}$, where $n = (-z + 2y)/x$. The overall pyrite oxidation reaction can then be written as (Descostes, 2001)

$$FeS_2 + \frac{6n+n'}{2n'}\ O_2 + \frac{2n-n'}{n'}\ H_2O \rightarrow Fe^{2+} + \frac{2n}{n'}SO_4^{2-} + \frac{2(n'-n)}{n'}\ S^0 + 2\left(\frac{2n-n'}{n'}\right)H^+. \quad (13)$$

Table 6 shows values of $R \leq 2$ for different possible values of n and n', where disproportion reactions are thermodynamically possible for different known sulfur species $S^{(n)}$ and $S^{(n')}$. Several ($S^{(n)}$, $S^{(n')}$) couples can theoretically generate $R \leq 2$. Among them, the ($S_2O_3^{2-}$; $S_4O_6^{2-}$) couple is plausible for several reasons:

(1) Thiosulfate has already been detected in such dissolution experiments in carbonated media (see Descostes et al., 2002);
(2) Thiosulfate has a mean number of oxidation equal to 2 and is thought to be the first aqueous sulfur species released from the pyrite surface (see Luther, 1987; Descostes et al., 2001; Rimstidt and Vaughan, 2003);
(3) Thiosulfate oxidation into tetrathionate is possible in only one elementary reaction since the number of transferred electrons is less than 2 (Basolo and Pearson, 1958);
(4) Thiosulfate and tetrathionate are expected to be metastable before the formation of sulfate ions under our experimental conditions (Fig. 7);
(5) The observed variation of R as a function of pH can be explained by the stability regions of pyrite, thiosulfate, elementary sulfur and tetrathionate. Thiosulfate ion is unstable in an acidic medium from pH = 3. It disproportion-

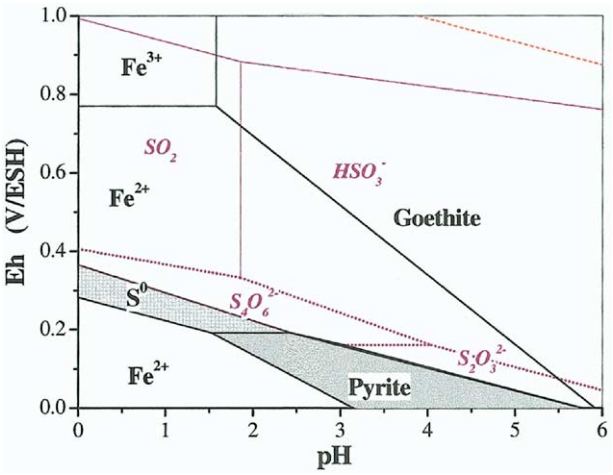

Fig. 7. Eh-pH diagram for the sulfur-iron-water system at 25°C, considering only sulfur species with an oxidation number below that of sulfate ($[\Sigma S] = 2 \times [\Sigma Fe] = 2.10^{-5}$ mol L^{-1}). See Descostes (2001) for thermodynamic data.

ates into S^0 and $S_4O_6^{2-}$. Tetrathionate ion would then be rapidly oxidized into sulfate. As pH decreases, the proportion of S^0 increases; the $[SO_4^{2-}]/[Fe]_{tot}$ ratio then decreases. However, as we will discuss below, this trend can also be explained by the degassing of SO_2.

The proposed pyrite oxidation process in an acidic medium can be summarized using the following reaction sequence, with a first step not involving acidification. Corresponding ΔG_R (see Descostes, 2001 for thermodynamic data) are also given. Firstly, surface disulfide hydrates and oxidizes, forming a thiosulfate moiety according to

$$\begin{gathered} FeS_2 + 3/2O_{2(g)} \rightarrow Fe^{2+} + S_2O_3^{2-} \\ \Delta G_R = -445.9 \text{ kJ mol}^{-1} \end{gathered} \quad (14)$$

Thiosulphate then disproportionates:

$$\begin{gathered} S_2O_3^{2-} + 6/5H^+ \rightarrow 2/5S^0 + 2/5S_4O_6^{2-} + 3/5H_2O \\ \Delta G_R = -36.0 \text{ kJ mol}^{-1} \end{gathered} \quad (15)$$

Tetrathionate further oxidizes, yielding both SO_4^{2-} and protons, according to

$$\begin{gathered} S_4O_6^{2-} + 7/2O_{2(g)} + 3H_2O \rightarrow 4SO_4^{2-} + 6H^+ \\ \Delta G_R = -1224.0 \text{ kJ mol}^{-1} \end{gathered} \quad (16)$$

Reaction 16 can tentatively be divided into two other intermediate steps with the production of sulfite (SO_3^{2-}), to respect the rule of a limited number of electrons being transferred and its observation in alkaline media (Descostes et al., 2002) according to:

$$\begin{gathered} S_4O_6^{2-} + 3/2O_{2(g)} + 3H_2O \rightarrow 4SO_3^{2-} + 6H^+ \\ \Delta G_R = -193.5 \text{ kJ mol}^{-1} \end{gathered} \quad (17)$$

and

$$\begin{gathered} SO_3^{2-} + 1/2O_2 \rightarrow SO_4^{2-} \\ \Delta G_R = -257.6 \text{ kJ mol}^{-1} \end{gathered} \quad (18)$$

Hence, the overall reaction (i.e. reaction 13 and R = 1.6) is

$$\begin{gathered} FeS_2 + 2.9O_{2(g)} + 0.6H_2O \rightarrow \\ Fe^{2+} + 0.4S^0 + 1.6SO_4^{2-} + 1.2H^+. \\ \Delta G_R = -971,5 \text{ kJ mol}^{-1} \end{gathered} \quad (19)$$

S^0 precipitation, as a consequence of thiosulfate disproportion is enough to explain the sulfur deficit observed in solution (Fig. 6). However, the expected R = 1.6 is greater than experimental R values under more acidic conditions. Therefore reaction 12 might not be complete, or another disproportion step need to be considered from, e.g., $S_3O_6^{2-}$, as proposed by Schippers et al. (1999) or sulfite (SO_3^{2-}). In the first case, a ratio equal to 1.20 is expected. A similar value is found when the first released sulfoxyanion considered is $S_5O_6^{2-}$. We prefer to assign ratios less than to 1.6 to sulfite. Thiosulfate, as we discussed before, is thought to be the first aqueous sulfur species released during the pyrite oxidation process. Moreover, SO_3^{2-} in acidic conditions is stable under SO_2 form (Fig. 7). If thiosulfate is the first aqueous species, then SO_2 formation in acidic conditions leads to the following net reaction:

$$FeS_2 + 2.1O_2 + 2H^+ \rightarrow Fe^{2+} + 0.4S^0 + 1.6SO_{2(g)} + H_2O, \quad (20)$$

and the R ratio calculated is then equal to 1.00. Hence, it is not out of the question that a partial degassing of SO_2 occurs in this case, which would tend to increase the aqueous sulfur deficit and lead to ratios between 1.6 and 1.00, depending on pH.

Full validation of this reaction model would require thiosulfate and tetrathionate ions to be detected in our solutions. However, these species are probably below current detection limits because of fast oxidation into sulfate in an acidic medium. Taylor et al. (1984) drew similar conclusions by observing no sulfur isotopic fractionation between sulfate ions and pyrite during its oxidation in oxygenated conditions. They interpreted this result as due to sulfoxyanion of very short lifetime during pyrite oxidation (or the absence of any intermediate, not consistent with many experimental observations).

A serious caveat to our model is the failure to detect S^0 precipitates at the pyrite surface, by XPS, by nuclear microprobe, or by observation of filtrates by SEM. We can possibly explain this by the small amounts of matter involved. In the case of the M21 experiment, if we considered the total amount of sulfur based on iron concentrations, sulfur S^0 in colloidal form would represent $1.8.10^{-6}$ mol L^{-1} at the end of the run, i.e., 32 ppm. Our estimated XPS detection limit is 1000 ppm. Also, elementary sulfur under vacuum conditions is volatile and tends to sublimate even at 270 K (Mycroft et al., 1990). However, McGuirre et al. (2001) also proposed the presence of elementary sulfur on an oxidized pyrite surface in an acidic medium (pH = 1 in sulfuric acid medium and in presence of 500 ppm of Fe^{3+}, duration = 96 h, T = 42°C). These authors have identified a heterogeneous distribution of oxidation products at the pyrite surface by Raman microscopy, as also observed by nuclear microprobe (Descostes et al., 2001).

In conclusion, assuming disproportion of thiosulfate ions into S^0 and $S_4O_6^{2-}$ is consistent with thermodynamic considerations (Charlot et al., 1959; Fig. 7) and mechanisms proposed by Luther (1997), Kelsall et al. (1999) and Rimstidt and Vaughan (2003). There is no need to assume preferential dissolution of iron in acidic media (Buckley and Woods, 1987; Mycroft et al., 1990; Sasaki et al., 1995; Zhu et al., 1994; Ahlberg and Broo, 1997). Sulfur deficit in acidic media has also been observed for dissolution experiment of duration greater than 24 h (experiment M22, R = 1.3).

This experimental approach followed here could be applied to most sulfide minerals, in particular to pyrrhotite ($Fe_{1-x}S$) which is known to dissolve with production of $H_2S_{(g)}$. In this latter case, disproportion and degassing reactions should complicate the reactional mechanism.

Acknowledgments—The support of the "Agence Nationale pour la gestion des Déchets Radioactifs" through grant FT00-1-066 is gratefully acknowledged. We thank Michel Schlegel of CEA for insightful comments on a previous version of the manuscript. The authors are grateful to the staff of Service d'Analyse des Roches et Minéraux (CNRS-CRPG, Service d'Analyse des Roches et Minéraux, Laboratoire de chimie, B. P. 20-54501, Vandoeuvre Cedex, France) for trace measurements. We thank an anonymous reviewer for its careful reading of the manuscript and the useful comments.

Associate editor: D. Vaughan

REFERENCES

Ahlberg E. and Broo A. E. (1997) Electrochemical reaction mechanisms at pyrite in acidic perchlorate solutions. *J. Electrochem. Soc.* **144,** 1281–1285.

Bailey L. K. and Peters E. (1976) Decomposition of pyrite in acids by pressure leaching and anodization: The case for an electrochemical mechanism. *Can. Metallurg. Q.***15,** 333–344.

Basolo F. and Pearson R. G. (1958) *Mechanisms of Inorganic Reactions: A Study of Metals Complexes in Solution.* Wiley.

Beaucaire C., Pitsch H., Toulhoat P., Motellier S., and Louvat D. (2000) Regional fluid characterisation and modelling of water-rock equilibria in the Boom clay Formation and in the Rupelian aquifer at Mol, Belgium. *Appl. Geochem.* **15,** 667–686.

Berner R. A. (1984) Sedimentary pyrite formation: An update. *Geochim. Cosmochim. Acta* **48,** 605–615.

Biegler T. and Swift D. A. (1979) Anodic behavior of pyrite in acid solutions. *Electrochim. Acta* **24,** 415–420.

Bonnissel-Gissinger P., Alnot M., Ehrhardt J.-J., and Behra P. (1998) Surface oxidation of pyrite as a function of pH. *Environ. Sci. Technol.* **32,** 2839–2845.

Buckley A. N. and Woods R. (1987) The surface oxidation of pyrite. *Appl. Surf. Sci.* **27,** 437–452.

Charlot G., Badoz-Lambling J., and Trémillon B. (1959) *Les réactions électrochimiques: Méthodes électrochimiques d'analyse*. Editions Masson & Cie, Paris.

Cruz R., Bertrand V., Monroy M., and Gonzalez I. (2001) Effect of sulfide impurities on the reactivity of pyrite and pyritic concentrates: A multi-tool approach. *Appl. Geochem.***16,** 803–819.

Descostes M. (2001) Evaluation d'une perturbation oxydante en milieu argileux: Mécanismes d'oxydation de la pyrite (FeS_2). Ph.D. thesis. Université Denis Diderot Paris VII.

Descostes M., Mercier F., Thromat N., Beaucaire C., and Gautier-Soyer M. (2000) Use of XPS to the determination of chemical environment and oxidation state of iron and sulfur samples. Constitution of a data basis in binding energies for Fe and S reference compounds and applications to the evidence of surface species of an oxidized pyrite in a carbonate medium. *Appl. Surf. Sci.* **165,** 288–302.

Descostes M., Mercier F., Beaucaire C., Zuddas P., and Trocellier P. (2001) Nature and distribution of chemical species on oxidized pyrite surface: Complementarity of XPS and nuclear microprobe analysis. *Nucl. Inst. Methods Phys. Res. B* **181,** 603–609.

Descostes M., Beaucaire C., Mercier F., Savoye S., Sow J., and Zuddas P. (2002) Effect of carbonate ions on pyrite (FeS_2) dissolution. *Bull. Soc. Geol. France* **173,** 265–270.

Donato P., Mustin C., Benoit R., and Erre R. (1993) Spatial distribution of iron and sulfur species on the surface of pyrite. *Appl. Surf. Sci.* **68,** 81–93.

Ennaoui A., Fiechter S., Jaegermann W., and Tributsch H. (1986) Photoelectrochemistry of highly quantum efficient single-crystalline n-FeS_2 (pyrite). *J. Electrochem. Soc.* **133,** 97–106.

Evangelou V. P. B. (1995) *Pyrite Oxidation and Its Control.* CRC Press.

Fornasiero D., Eijt V., and Ralston J. (1992) An electrokinetic study of pyrite oxidation. *Colloids Surf.* **62,** 63–73.

Garrels R. M. and Thomson M. E. (1960) Oxidation of pyrite by iron sulfate solutions. *Am. J. Sci.*57–67.

Goldhaber M. B. (1983) Experimental study of metastable sulfur oxyanion formation during pyrite oxidation at pH 6–9 and 30°C. *Am. J. Sci.* **238,** 193–217.

Guevremont J. M., Elsetinow A. R., Strongin D. R., Bebie J., and Schoonen M. A. A. (1998) Structure sensitivity of pyrite oxidation: Comparison of the (100) and (111) planes. *Am. Mineral.* **83,** 1353–1356.

Ichikuni P. M. (1960) Sur la dissolution des minerais sulfurés en divers milieux. *Bull. Chem. Soc. Jpn.* **33,** 1052–1057.

Kamei G. and Ohmoto H. (2000) The kinetics of reactions between pyrite and O_2-bearing water revealed from in situ monitoring DO, Eh and pH in a closed system. *Geochim. Cosmochim. Acta* **64,** 2585–2601.

Kelsall G. H., Yin Q., Vaughan D. J., England K. E. R., and Brandon N. P. (1999) Electrochemical oxidation of pyrite (FeS_2) in aqueous electrolytes. *J. Electroanalyt. Chem.* **471,** 116–125.

Knipe S. W., Mycroft J. R., Pratt A. R., Nesbitt H. W., and Bancroft G. M. (1995) X-ray photoelectron spectroscopy study of water adsorption on iron sulphide minerals. *Geochim. Cosmochim. Acta* **59,** 1079–1090.

Luther G. W. III. (1987) Pyrite oxidation and reduction: Molecular orbital theory considerations. *Geochim. Cosmochim. Acta* **51,** 3193–3199.

Luther G. W. III. (1997) Comment on "Confirmation of a sulfur-rich layer on pyrite after oxidative dissolution by Fe(III) ions around pH 2" by K. Sasaki, M. Tsunekawa, S. Tanaka, and H. Konno. *Geochim. Cosmochim. Acta* **61,** 3269–3271.

McClendon J. H. (1999) The origin of life. *Earth-Sci. Rev.* **47,** 71–93.

McGuirre M. M., Jallad K. N., Ben-Amotz D., and Hamers R. J. (2001) Chemical mapping of elemental sulfur on pyrite and arsenopyrite surfaces using near-infrared Raman imaging microscopy. *Appl. Surf. Sci.* **178,** 105–115.

McKibben M. A. and Barnes H. L. (1986) Oxidation of pyrite in low temperature acidic solutions: Rate laws and surface textures. *Geochim. Cosmochim. Acta* **50,** 1509–1520.

Moses C. O., Nordstrom D. K., Herman J. S., and Mills A. L. (1987) Aqueous pyrite oxidation by dissolved oxygen and ferric iron. *Geochim. Cosmochim. Acta* **51,** 1561–1571.

Motellier S., Gurdale K., and Pitsch H. (1997) Sulfur speciation by capillary electrophosis with indirect spectrophotometric detection: In search of a suitable carrier electrolyte to maximize sensitivity. *J. Chromatogr. A* **770,** 311–319.

Motellier S. and Descostes M. (2001) Sulfur speciation and tetrathionate sulfitolysis monitoring by capillary electrophosis. *J. Chromatogr. A* **907,** 329–335.

Mycroft J. R., Mcintyre N. S., Lorimer J. W., and Hill I. R. (1990) Detection of sulfur and polysulphides on electrochemically oxidized pyrite surfaces by X-ray photoelectron spectroscopy and Raman spectroscopy. *J. Electranal. Chem.* **292,** 139–152.

Nesbitt H. W., Scaini M. J., Höchst H., Bancroft G. M., Schaufuss A. G., and Szargan R. (2000) Synchrotron XPS evidence for Fe^{2+}-S and Fe^{3+}-S surface species on pyrite fracture-surfaces, and their 3D electonic states. *Am. Mineral.* **85,** 850–857.

Nicholson R. V., Gillham R. W., and Reardon E. J. (1988) Pyrite oxidation in carbonate-buffered solution: 1. Experimental kinetics. *Geochim. Cosmochim. Acta* **52,** 1077–1085.

Nicholson R. V., Gillham R. W., and Reardon E. J. (1990) Pyrite oxidation in carbonate-buffered solution: 2. Rate control by oxide coatings. *Geochim. Cosmochim. Acta* **54,** 395–402.

Pain D. J., Sanchez A., and Meharg A. A. (1998) The Doñana ecological disaster: Contamination of a world heritage estuarine marsh ecosystem with acidified pyrite mine waste. *Sci. Total Environ.* **222,** 45–54.

Rich R. A., Holland H. D., and Petersen U. (1977) Hydrothermal uranium deposits. In *Developments in Economic Geology,*Vol. 6. Elsevier.

Rimstidt J. D. and Vaughan D. J. (2003) Pyrite oxidation: A state-of-the-art assessment of the reaction mechanism. *Geochim. Cosmochim. Acta* **67,** 873–880.

Rosso K. M., Becker U., and Hochella M. F. Jr. (1999a) Atomically resolved electronic structure of pyrite {100} surfaces: An experimental and theoretical investigation with implications for reactivity. *Am. Mineral.* **84,** 1535–1548.

Rosso K. M., Becker U., and Hochella M. F. Jr. (1999b) The interaction of pyrite {100} surfaces with O_2 and H_2O: Fundamental oxidation mechanisms. *Am. Mineral.* **84,** 1549–1561.

Sasaki K., Tsunekawa M., Tanaka S., and Konno H. (1995) Confirmation of a sulfur-rich layer on pyrite after oxidative dissolution by Fe(III) ions around pH 2. *Geochim. Cosmochim. Acta* **59,** 3155–3158.

Sasaki K., Tsunekawa M., Tanaka S., and Konno H. (1997) Reply to the comment by G. W. Luther III on "Confirmation of a sulfur-rich layer on pyrite after oxidative dissolution by Fe(III) ions around pH 2." *Geochim. Cosmochim. Acta* **61,** 3273–3274.

Scaini M. J., Bancroft G. M., and Knipe S. W. (1997) An XPS, AES, and SEM study of the interactions of gold and silver chloride

species with PbS and FeS_2: Comparison to natural samples. *Geochim. Cosmochim. Acta* **61,** 1223–1231.

Schaufuss A. G., Nesbitt H. W., Kartio I., Laajalehto K., Bancroft G. M., and Szargan R. (1998) Reactivity of surface chemical states on fractured pyrite. *Surf. Sci.* **411,** 321–328.

Schippers A., Rohwerder T., and Sand W. (1999) Intermediary sulfur compounds in pyrite oxidation: Implications for bioleaching and biodepyritization of coal. *Appl. Microbiol. Biotechnol.* 52, 104–110.

Singer P. C. and Stumm W. (1970) Acid mine drainage: The rate-limiting step. *Science* **167,** 1121–1123.

Steger H. F. and Desjardins L. E. (1978) Oxidation of sulfide minerals, 4. Pyrite, chalcopyrite and pyrrhotite. *Chem. Geol.* **23,** 225–237.

Taylor B. E., Wheeler M. C., and Nordstrom D. K. (1984) Stable isotope geochemistry of acid mine drainage: Experimental oxidation of pyrite. *Geochim. Cosmochim. Acta* **48,** 2669–2678.

Toniazzo V., Mustin C., Portal J. M., Humbert B., and Erre R. (1999) Elemental sulfur at the pyrite surfaces: Speciation and quantification. *Appl. Surf. Sci.* **143,** 229–237.

Uhlig I., Szargan R., Nesbitt H. W., and Laajalehto K. (2001) Surface states and reactivity of pyrite and marcasite. *Appl. Surf. Sci.* **179,** 222–229.

Viollier E., Inglett P. W., Hunter K., Roychoudhury A. N., and Van Cappellen P. (2000) The ferrozine method revisited: Fe(II)/Fe(III) determination in natural waters. *Appl. Geochem.* **15,** 785–790.

Wächtershäuser G. (2000) Life as we don't know it. *Science* **289,** 1307–1308.

Wei D. and Osseo-Asare K. (1997) Semiconductor electrochemistry of particulate pyrite mechanisms and products of dissolution. *J. Electrochem. Soc.* **144,** 546–553.

Williamson M. A. and Rimstidt J. D. (1994) The kinetics and electrochemical rate-determining step of aqueous pyrite oxydation. *Geochim. Cosmochim. Acta* **58,** 5443–5454.

Zhu X., Li J., and Wadsworth M. E. (1994) Characterization of surface layers formed during pyrite oxidation. *Colloids Surf. A***93,** 201–210.